Clusters and the Cosmic Web

Weygaert, R. van de

Published in:
Physical Review D

Publication date:
2006

CLUSTERS AND THE COSMIC WEB:
Identifying the location of filaments

Rien van de Weygaert
Kapteyn Astronomical Institute, University of Groningen, P.O. Box 800, 9700 AV Groningen, the Netherlands

Introduction

The interior of the Universe is permeated by a tenuous space-filling frothy network. Welded into a distinctive foamy pattern, galaxies accumulate in walls, filaments and dense compact clusters surrounding large near-empty void regions. As borne out by a large sequence of computer experiments, such weblike patterns in the overall cosmic matter distribution do represent a universal but possibly transient phase in the gravitationally propelled emergence and evolution of cosmic structure. In this contribution we discuss the intimate relationship between the filamentary features and the rare dense compact cluster nodes in this network, via the large scale tidal field going along with them (see fig 1), following the *cosmic web* theory developed by Bond et al. (1996). The Megaparsec scale tidal shear pattern is responsible for the contraction of matter into filaments, and its link with the cluster locations can be understood through the implied quadrupolar mass distribution in which the clusters are to be found at the sites of the overdense patches (Van de Weygaert et al. 1996)). The pattern of the cosmic web can therefore be largely tied in with the protocluster peaks in the primordial density field, and the subsequent nonlinear evolution leads to the aggregation of matter into the sharp filamentary network defined by the primordial tidal shear field.

We present a new technique for tracing the cosmic web, identifying planar walls, elongated filaments and cluster nodes in the galaxy distribution. These will allow the practical exploitation of the concept of the cosmic web towards identifying and tracing the locations of the gaseous WHIM. These methods, the Delaunay Tessellation Field Estimator and the Morphology Multiscale Filter (Schaap & van de Weygaert 2000; Aragón-Calvo et al. 2006), find their basis in computational geometry and visualization.

1 Anisotropic Collapse

A major characteristic of the formation of cosmic structure in gravitational instability scenarios is the tendency of matter concentrations to collapse in an *anisotropic* manner. In a generic random density field the gravitational force field at any location will be anisotropic. For a particular structure the *internal* force field of the structure hangs together with the flattening of the feature itself. It induces an anisotropic collapse along the main axes of the structure. In reality, the internal evolution of the system will be dominated by internal substructure involving a substantial measure of orbit crossing. The more quiescent *external 'background' force field*, the integrated gravitational impact of all external density features in the Universe will also be *anisotropic*.

In all, the resulting evolution can be most clearly understood in and around a density maximum (or minimum) δ, to first order corresponding to the collapse of a homogeneous ellipsoid (Icke 1973; Eisenstein & Loeb 1995; Bond & Myers 1996), as illustrated in fig. 2. The

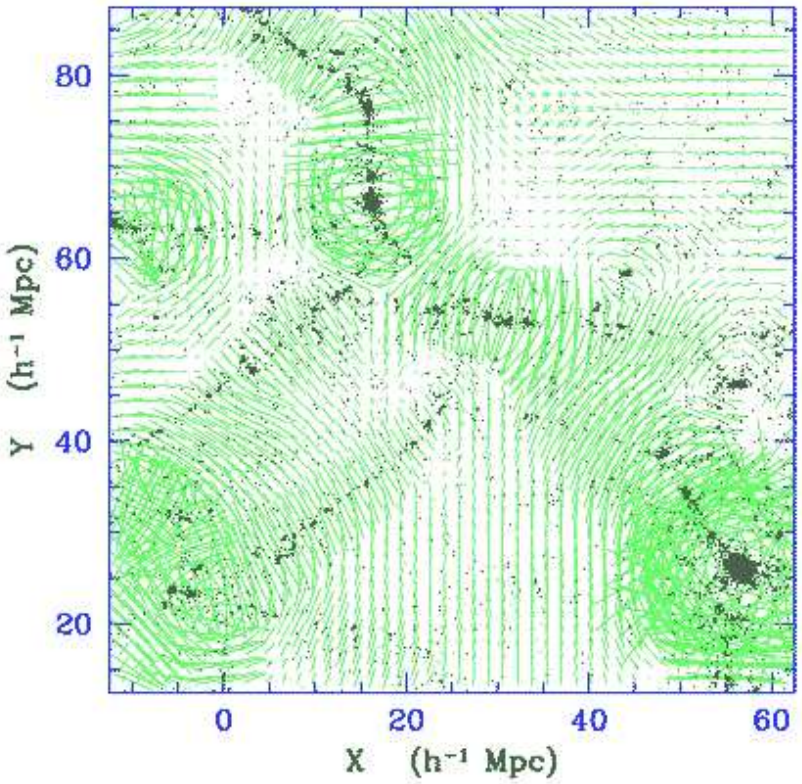

Figure 1: The relation between the *cosmic web*, the clusters at the nodes in this network and the corresponding compressional tidal field pattern. It shows the matter distribution at the present cosmic epoch, along with the (compressional component) tidal field bars in a slice through a simulation box containing a realization of cosmic structure formed in an open, $\Omega_\circ = 0.3$, Universe for a CDM structure formation scenario (scale: $R_G = 2h^{-1}$Mpc). The frame shows structure in a $5h^{-1}$Mpc thin central slice, on which the related tidal bar configuration is superimposed. The matter distribution, displaying a pronounced weblike geometry, is clearly intimately linked with a characteristic coherent compressional tidal bar pattern. From: Van de Weygaert (2002)

overall characteristics can also be understood for the more generic circumstances of a density fluctuation field, where the early phases of the collapse of a feature may be approximated by the Zel'dovich deformation tensor ψ_{mn} (Zel'dovich 1970). Related to the total *tidal force field* T_{mn} acting over a patch of density excess δ, including the contributions from the local ("internal") flattening of the density field as well as those generated by external density perturbations, the eigenvalues λ_1, λ_2 and λ_3 of the deformation tensor ψ_{mn},

$$\psi_{mn} \;=\; \frac{2}{3a^3\Omega H^2}\,\frac{\partial^2 \underline{\phi}}{\partial q_m \partial q_n} \;=\; \frac{1}{\frac{3}{2}\Omega H^2 a}\Big(\,\underline{T}_{mn} \;+\; \frac{1}{2}\Omega H^2\,\underline{\delta}\,\delta_{mn}\,\Big) \qquad (1)$$

(underlined quantities are the linearly extrapolated values). Dependent on whether one or more of the eigenvalues $\lambda_i > 0$, the feature will collapse along one or more directions. The collapse will proceed along a sequence of three stages. First, collapse along the direction of the strongest deformation λ_1. The feature will be like a *wall*, flattened. If also the second eigenvalue is positive, the object will contract along the second direction and an elongated *filamentary* structure results. Total collapse will occur if also $\lambda_3 > 0$. In N-body simulations as well as in galaxy redshift distributions it are in particular the filaments which stand out as the most prominent feature of the *Cosmic Web*. It even remains unclear whether *walls* are even present at all. Some argue that once nonlinear clustering sets in the stage in which walls form is of

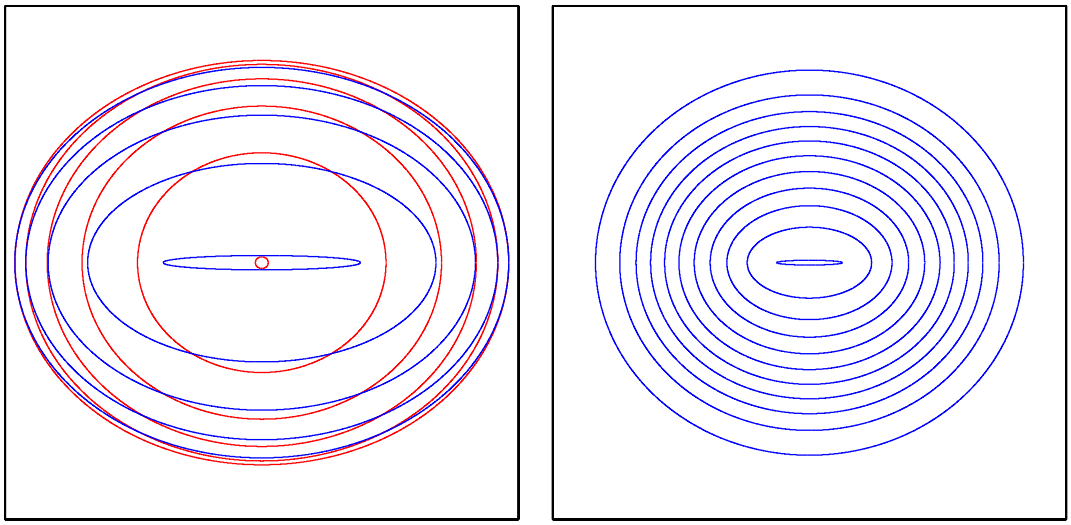

Figure 2: The evolution of an overdense homogeneous ellipsoid, with initial axis ratio $a_1 : a_2 : a_3 = 1.0 : 0.9 : 0.9$, embedded in an Einstein-de-Sitter background Universe. The two frames show a time sequel of the ellipsoidal configurations attained by the object, starting from a near-spherical shape, initially trailing the global cosmic expansion, and after reaching a maximum expansion turning around and proceeding inexorably towards ultimate collapse as a highly elongated ellipsoid. Left: the evolution depicted in physical coordinates. Red contours represent the stages of expansion, blue those of the subsequent collapse after turn-around. Right: the evolution of the same object in comoving coordinates, a monologous procession through ever more compact and more elongated configurations.

a very short duration or does not occur at all: true collapse would proceed along filamentary structures (Sathyaprakash et al. 1996; Jain & Bertschinger 1994; Hui & Bertschinger 1996). Indeed, it can be argued that the typical density contours of overdense regions subject to tidal shear constraints are already more filamentary than sheet-like in the linear density field, and becomes even more so in the quasi-linear regime (Bond et al. 1996). In addition, there is also a practical problem in identifying them, due to walls having a far lower surface density than the filaments. This is exacerbated as there are hardly any objective feature detection techniques available available. Very recent results based upon the analysis of an N-body simulation of cosmic structure formation by means of the new Multiscale Morphology Filter technique indeed identified walls in abundance whether they had not been seen before (Aragón-Calvo et al. 2006). Another indication is that the dissipative gaseous matter within the cosmic web indeed partially aggregates in walls with low overdensities (Kang et al. 2005; Kang 2006), arguing for the presence of moderate potential wells tied in with dark matter walls.

2 Cosmic Web: Tides and Quadrupoles

Bond, Kofman & Pogosyan (1996) coined the word 'cosmic web' in their study of the physical content of the web, in which they drew attention to their observation that knowledge of the value of the tidal field at a few well-chosen cosmic locations in some region would determine the overall outline of the weblike pattern in that region. This relation may be traced back to a simple configuration, that of a "global" quadrupolar matter distribution and the resulting "local" tidal shear at a particular location $\mathbf{r}$. Such a quadrupolar primordial matter distribution will almost by default evolve into the canonical cluster-filament-cluster configuration which appears so prominently in the cosmic foam (see fig 3). For a cosmological (random) matter distribution

this close connection between local force field and global matter distribution may be elucidated through the expression of the tidal tensor in terms of the generating cosmic matter density fluctuation distribution $\delta(\mathbf{r})$ (Van de Weygaert et al. 1996):

$$T_{ij}(\mathbf{r}) \;=\; \frac{3\Omega H^2}{8\pi} \int \mathrm{d}\mathbf{r}'\, \delta(\mathbf{r}') \; \left\{ \frac{3(r'_i - r_i)(r'_j - r_j) - |\mathbf{r}' - \mathbf{r}|^2 \; \delta_{ij}}{|\mathbf{r}' - \mathbf{r}|^5} \right\} \; - \\ - \; \frac{1}{2}\Omega H^2 \; \delta(\mathbf{r}, t) \; \delta_{ij} \tag{2}$$

3 Constrained Random Field Formalism

The set of density field realizations $\delta(\mathbf{r})$ within a sample volume $\mathcal{V}_s$ that would generate a tidal field T_{ij} at location $\mathbf{r}$ can be inferred from the theory of constrained random fields (Bertschinger 1987). Bertschinger described how a set Γ of functional field constraints $C_i[f] = c_i$, $(i = 1, \ldots, M)$ of a Gaussian random field $f(\mathbf{r}, t)$ would translate into field configurations for which these constraints would indeed have the specified values c_i. Any such *constrained field realization* f_c can be written as the sum of a *mean field* $\bar{f}(\mathbf{x}) = \langle f(\mathbf{x})|\Gamma\rangle$, the ensemble average of all field realizations obeying the constraints, and a *residual field* $F(\mathbf{x})$, embodying the field fluctuations characterized and specified by the power spectrum $P(k)$ of the particular cosmological scenario at hand,

$$f_c(\mathbf{x}) \;=\; \bar{f}(\mathbf{x}) \;+\; F(\mathbf{x}) \tag{3}$$

Bertschinger(1987) showed the specific dependence of the mean field on the *nature* $C_i[f]$ of the constraints as well as their *values* c_i. In essence the mean field can be seen as the weighted sum of the field-constraint correlation functions $\xi_i(\mathbf{x}) \equiv \langle f\, C_i\rangle$ (where we follow the notation of Hoffman & Ribak (1991)). Each field-constraint correlation function encapsulates the repercussion of a specific constraint $C_i[f]$ for a field $f(\mathbf{x})$ throughout the sample volume $\mathcal{V}_s$. Not surprisingly, the field-constraint correlation function for the tidal constraint T_{ij} is a quadrupolar configuration. The weights for each of the relevant $\xi_i(\mathbf{x})$ are determined by the value of the constraints, c_m, and their mutual cross-correlation $\xi_{mn} \equiv \langle C_m C_n\rangle$,

$$\bar{f}(\mathbf{x}) \;=\; \xi_i(\mathbf{x})\, \xi^{-1}_{ij}\, c_j \,. \tag{4}$$

Generating the residual field F is a nontrivial exercise: the specified constraints translate into locally fixed phase correlations. This renders a straightforward random phase Gaussian field generation procedure unfeasible. Hoffman & Ribak (1991) pointed out that for a Gaussian random field the sampling is straightforward and direct, which greatly faciliated the application of CRFs to cosmological circumstances. This greatly facilitated the application of CRFs to complex cosmological issues (Klypin et al. 2003; Mathis et al. 2002). Van de Weygaert & Bertschinger (1996), following the Hoffman-Ribak formalism, worked out the specific CRF application for the circumstance of sets of local density peak (shape, orientation, profile) and gravity field constraints. With most calculations set in Fourier space, the constrained field realization for a linear cosmological density field with power spectrum $P(k)$ can be computed from the Fourier integral

$$f(\mathbf{x}) \;=\; \int \frac{\mathrm{d}\mathbf{k}}{(2\pi)^3} \left[\hat{\tilde{f}}(\mathbf{k}) + P(k)\, \hat{H}_i(\mathbf{k})\, \xi^{-1}_{ij}\, (c_j - \tilde{c}_j) \right] \mathrm{e}^{-\mathrm{i}\mathbf{k}\cdot\mathbf{x}} \tag{5}$$

with $\hat{H}_i(\mathbf{k})$ the constraint i's kernel (the Fourier transform of constraint $C_i[f]$), c_j the value of this constraint, while the tilde indicates it concerns a regular unconstrained field realization $\tilde{f}$. While the CRF formalism is rather straightforward for idealized linear constraints, reality is less forthcoming. If the constraints are based on measured data these will in general be noisy, sparse and incomplete. Wiener filtering will be able to deal with such a situation and reconstruct the

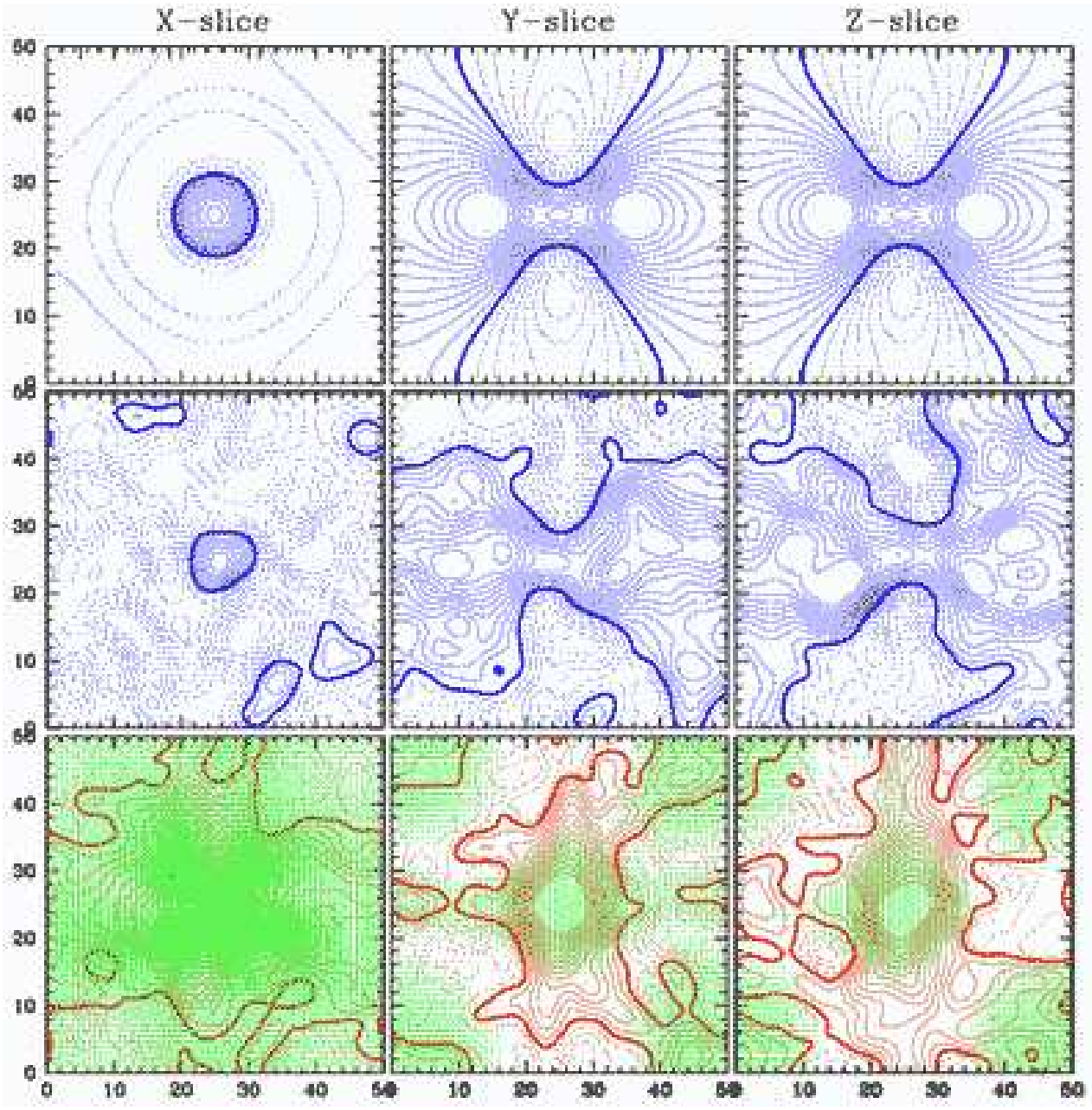

Figure 3: Constrained field construction of initial quadrupolar density pattern in a SCDM cosmological scenario. The tidal shear constraint is specified at the box centre location, issued on a Gaussian scale of $R_G = 2h^{-1}$Mpc and includes a stretching tidal component along the x- and y-axis acting on a small density peak at the centre. Its ramifications are illustrated by means of three mutually perpendicular slices through the centre. Top row: the "mean" field density pattern, the pure signal implied by the specified constraint. Notice the clear quadrupolar pattern in the y- and z-slice,directed along the x- and y-axis, and the corresponding compact circular density contours in the x-slice: the precursor of a filament. Central row: the full constrained field realization, including a realization of appropriately added SCDM density perturbations. Bottom row: the corresponding tidal field pattern in the same three slices. The (red) contours depict the run of the tidal field strenght $|T|$, while the (green) tidal bars represent direction and magnitude of the *compressional* tidal component in each slice (scale: $R_G = 2h^{-1}$Mpc). From: Van de Weygaert (2002)

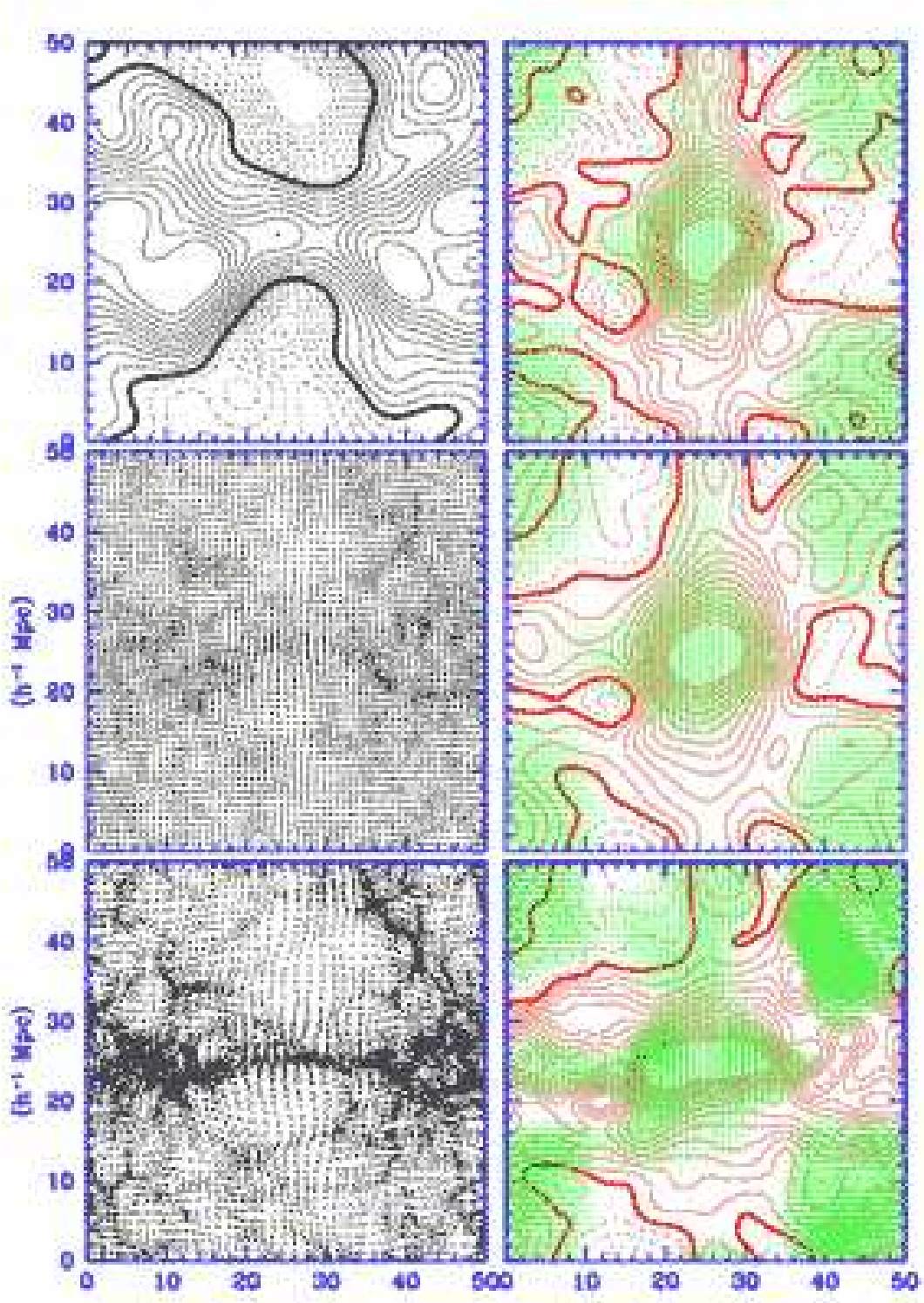

Figure 4: The emergence of a filament in an SCDM structure formation scenario. Lefthand column: density/particle distribution in z-slice through the centre of the simulation box. Right-hand column: the corresponding tidal field configurations, represented through the full tidal field strength $|T|$ contour maps (red), as well as the corresponding compressional tidal bars (scale: $R_G = 2h^{-1}$Mpc). From top to bottom: primordial field, $a = 0.2$ (visible emergence filament), present epoch. Note the formation of the filament at the site where the tidal forces peaked in strength, with a tidal pattern whose topology remains roughly similar. From: Van de Weygaert (2002)

implied *mean field*, at the cost of losing signal proportional to the loss in data quality (see e.g. **?**). A major practical limitation concerns the condition that the constrained field is Gaussian. For more generic nonlinear clustering situations the formalism is in need of additional modifications. For specific situations this may be feasible (Sheth 1995), but for more generic circumstances this is less obvious (however, see Jones & van de Weygaert (2006)).

4 Tidal connections: Filaments and Clusters

One of the major virtues of the *constrained random field* construction technique is that it offers the instrument for translating locally specified quantities into the corresponding implied global matter distributions for a given structure formation scenario. In principle, the choice of possible implied matter distribution configurations is limitless, yet it gets substantially curtailed by the statistical nature of its density fluctuations, the coherence scale of the matter distribution and hence of the generated force field as well as the noise characteristics over the various spatial scales, both set by the power spectrum of fluctuations. Van de Weygaert & Bertschinger (1996) illustrate the repercussion of a specified constraint on the value of the tidal shear at some specific location. Figure 4 shows the result of such a tidal constraint. It provides a 3-D impression of the structure in the region immediately surrounding the location of the specified shear. We have crudely included the concept of "external" by (spherically) filtering the field on a (rather arbitrary) scale of $2h^{-1}$Mpc.

The *mean field* $\bar{f}$ of the specified constraints (top panels) represents a clear depiction of the average density field configuration inducing the specified tidal tensor: the constraint works out into a perfect global quadrupolar field. Superimposing the *residual* power spectrum fluctuations F, whose amplitude is modified by the local correlation with the specified constraints, results into a representative individual realization of a matter density distribution that would induce the specified constraint (second row). The close affiliation with a strong anisotropic force field, within the surrounding region, can be directly observed from the lower row of corresponding slices. The contour maps, indicating the total tidal field strength, reveal that the constraints correspond to a tidal field elongated along the axis of the box with a maximum tidal strength at the centre of the box. Along the full length of the filament we observe a coherent pattern of strong compressional forces perpendicular to its axis[1]. Assessing the evolution of the spatial

matter distribution in and around the (proto)filament, see Fig. 4, demonstrates the intimate correlation between the anisotropy in the cosmic force field and the presence of strongly anisotropic features. It shows the emergence of a filament in a CDM structure formation scenario, with the density//particle distribution along the "spine" of the emerging filament in the lefthand column and the corresponding tidal configuration (full tidal field strength contour map as well as corresponding bars of compressional tidal component) in the righthand column. The top row corresponds to the primordial cosmic conditions, the centre row to $a = 0.2$ and the bottom row to $a = 0.8$. At $a = 0.2$ we can clearly recognize the onset of the emerging filament, which at $a = 0.8$ has emerged as the dominant feature in the mass distribution. Two striking aspects of the depicted evolution are particularly relevant for this contribution:

[1]on the basis of the effect of a tidal field, we may distinguish at any one location between "compressional" and "dilational" components. Along the direction of a "compressional" tidal component T_c (for which $T_c < 0.0$) the resulting force field will lead to contraction, pulling together the matter currents. The "dilational" (or "stretching") tidal component T_d, on the other hand, represents the direction along which matter currents tend to get stretched as $T_d > 0$. Note that within a plane, cutting through the 3-D tidal "ellipsoid", the tidal field can consist of two compressional components, two dilational ones or – the most frequently encountered situation – of one dilational and one compressional component.

- Two *massive clusters* emerge on either side of the filament. These matter assemblies, in conjunction with the correspondingly large underdense volumes surrounding the filament perpendicular to its spinal axis, define a roughly quadrupolar density field and are a natural consequence of the primordial density field suggested by the central tidal force field constraint (fig. 3).

- The strong correlation between the compressional component of the tidal field and the presence of a dense filamentary feature suggests a strong causal link (fig. 1, 4). A comparison between the evolving cosmic web and the corresponding tidal force field, specifically of its compressional components, does suggest an intimate link. While the spatial pattern of the tidal field remains quite close to its primordial configuration, we see the formation of the filament precisely there where the primordial compressional field is very strong and coherent. In other words, it is as if *the primordial mapping of the compressional tidal component represents a prediction for the locus of the main cosmic web features.* The gradual emergence of one particular filament is seemingly predestinated by the tidal field configuration.

5 Tidal connections: Clusters and the Web

Inverting the relation between clusters and the cosmic web, we may investigate the repercussions of imposing the locations and nature of cluster nodes to trace out the implied cosmic web. This has been described in detail in Bond et al. (1996). Clusters are defined according to the peak-patch formalism of Bond & Myers (1996): they are peaks in the primordial Gaussian field, identified with the peak on the largest smoothing scale R_G on which they have collapsed along all three directions (according to the homogeneous ellipsoidal model).

As argued in the above, the presence of two protocluster peaks may imply that the tidal shear field configuration in between the peaks is such that a filament will form along the axis connecting the two clusters. The strength of the filamentary bridge depends on the distance between the two peaks. Its coherence and strength are set by the field-constraint correlation function $\xi_k(\mathbf{r}) = \langle \delta(\mathbf{r}) T_{ij}(\mathbf{r_T}) \rangle$ between the density field and the tidal shear. The strength of the correlation will depend strongly on both orientation and of the clusters and their mutual distance (Bond et al. (1996), also see Van de Weygaert et al. (1996)). This was indeed confirmed in a study of fully evolved intracluster filaments in GIF simulations (Colberg et al. 2005). In the observed galaxy distribution, "superclusters" are therefore filamentary cluster-cluster bridges, and the most pronounced ones will be found between clusters of galaxies that are close together and which are aligned with each other. Very pronounced galaxy filaments, the Pisces-Perseus supercluster chain is a telling example, are therefore almost inescapably tied in with a high concentration of rich galaxy clusters.

These observations can provide the path towards an efficient tracing of weblike patterns at higher redshifts. Clusters of galaxies are observable out to high redshifts $z > 1$. Using the cluster distribution within a particular cosmic region as input, the CRF technique will allow the reconstruction of the corresponding filamentary weblike patterns. This in turn may focus attention on the highest density patches for tracing the intergalactic gas and thus suggest an efficient observational technique. In turn, it will allow a test of structure formation.

6 Clusters and Filaments: Identification

Astronomical applications are usually based upon a set of user-defined filter functions. Nearly without exception the definition of these include pre-conceived knowledge about the features one is looking for. A telling example is the use of a Gaussian filter. This filter will suppress the presence of any structures on a scale smaller than the characteristic filter scale. Moreover, nearly

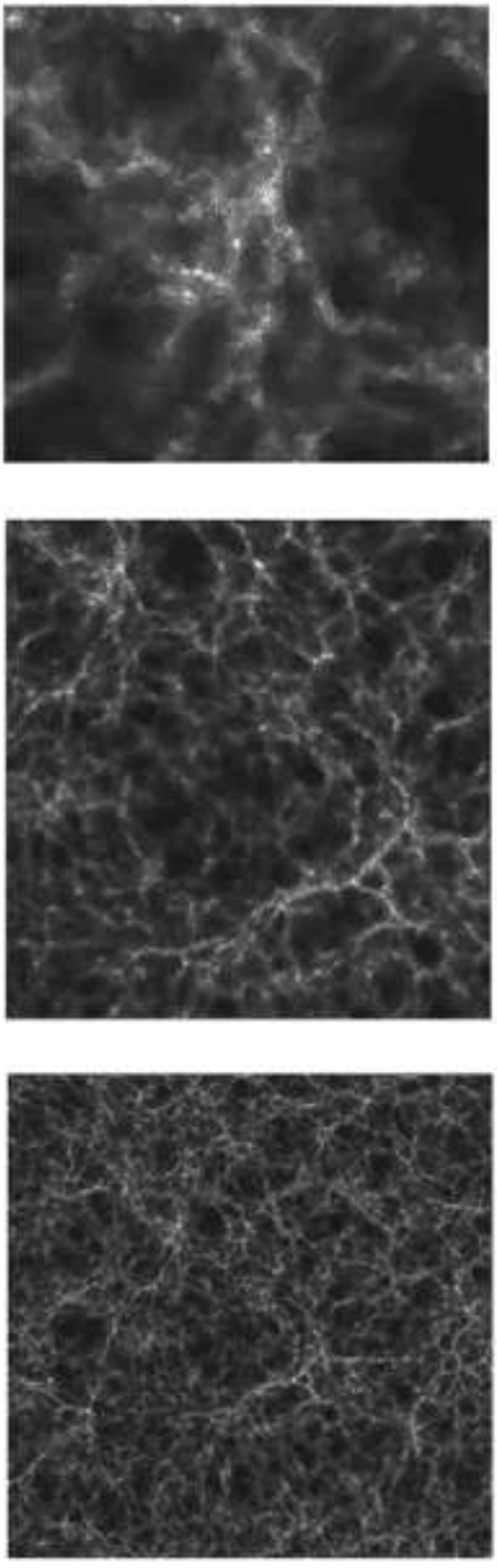

Figure 5: The Cosmic Web in a box: GIF N-body simulation of structure formation in a ΛCDM cosmology. Three consecutive zoom-ins onto a central slice through the simulation box. Courtesy: Willem Schaap.

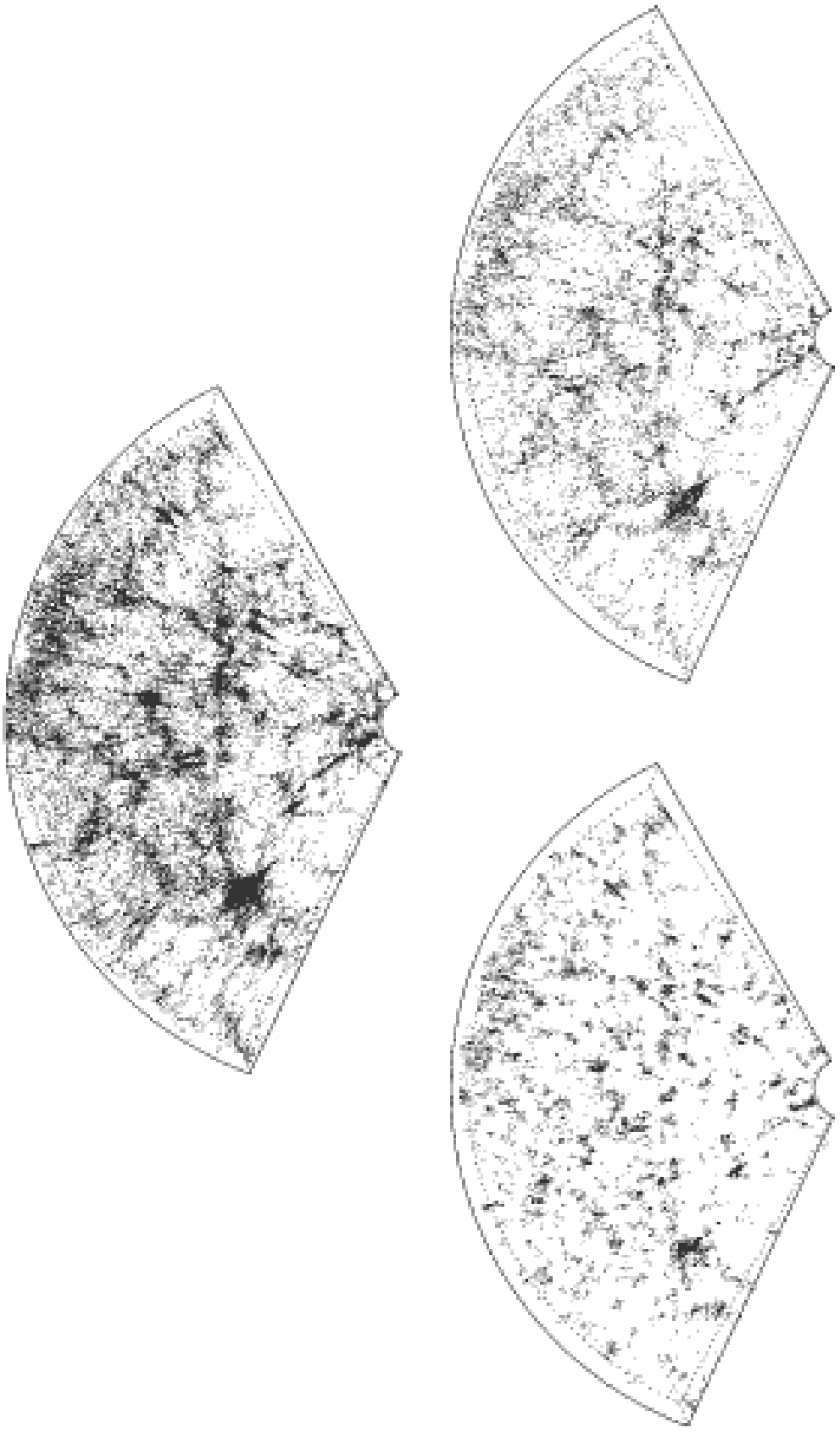

Figure 6: MMF (multiscale morphology filter) analysis of a slice in te SDSS survey. From the full galaxy distribution (left), the MMF identifies the galaxies belonging to clusters (top right) and to filaments (bottom right). From: Aragón-Calvo et al. (2006)

always it is a spherically defined filter which tends to smooth out any existing anisotropies. Such procedures may be justified in situations in which we are particularly interested in objects of that size or in which physical understanding suggests the smoothing scale to be of particular significance. On the other hand, they may be crucially inept in situations of which we do not know in advance the properties of the matter distribution. The gravitational clustering process in the case of hierarchical cosmic structure formation scenarios is a particularly notorious case. As it includes structures over a vast range of scales and displays a rich palet of geometries and patterns any filter design tends to involve a discrimination against one or more – and possibly interesting – characteristics of the cosmic matter distribution it would be preferrable to define filter and reconstruction procedures that tend to be defined by the discrete point process itself.

Here we exploit the potential of spatial **tessellations** as a means of estimating and interpolating discrete point samples into continuous field reconstructions, in particular that of *Voronoi* and *Delaunay tessellations* . Both tessellations – each others *dual* – are fundamental concepts in the field of stochastic geometry. They formed the basis of the technique of the Delaunay Tessellation Field Estimator (DTFE), defined and introduced by Schaap & van de Weygaert (2000). The DTFE technique is capable of delineating the hierarchical and anisotropic nature of spatial point distributions and in outlining the presence and shape of voidlike regions. It is precisely this which marks the spatial structure of the cosmic web. DTFE is based upon the use of the Voronoi and Delaunay tessellations of a given spatial point distribution to form the basis of a natural, fully self-adaptive filter for discretely sampled fields in which the Delaunay tessellations are used as multidimensional interpolation intervals. DTFE exploits two particular properties of Voronoi and Delaunay tessellations. The tessellations are very sensitive to the local point density, in that the volume of the tessellation cells is a strong function of the local (physical) density. The DTFE method uses this fact to define a local estimate of the density. It subsequently uses the adaptive and minimum triangulation properties of Delaunay tessellations to use them as adaptive spatial interpolation intervals for irregular point distributions. In this it is the first order version of the *Natural Neighbour method* (NN method). The theoretical basis for the NN method, a generic smooth and local higher order spatial interpolation technique developed by experts in the field of computational geometry, has been worked out in great detail by (Sibson 1980, 1981; Watson 1992). As has been demonstrated by telling examples in geophysics (Sambridge et al. 1995) and solid mechanics and engineering (Sukumar 1998) NN methods hold tremendous potential for grid-independent analysis and computations. The performance of DTFE may be appreciated from fig. 5. It clearly produces a continuous density field that includes, both qualititatively and quantitatively, all essential information of the underlying cosmic web. Based on this optimized

cosmic web reconstruction Aragón-Calvo et al. Aragón-Calvo et al. (2006) developed the Multiscale Morphology Filtere technique, particularly oriented towards recognizing and identifying the major characteristic elements in the Megaparsec matter density field. The MMF yields a unique framework for the combined identification of dense, compact bloblike clusters, of the salient and moderately dense elongated filaments and of tenuous planar walls. Of fundamental importance is the use of a morphologically unbiased and optimized continuous density field retaining all features visible in a discrete galaxy or particle distribution. This is accomplished by means of DTFE.

It is based upon an assessment of the coherence of a density (or intensity) field along a range of spatial scales and with the virtue of providing a generic framework for characterizing the local morphology of the density field and enabling the selection of those morphological features which the analysis at hand seeks to study. The technology finds its origin in computer vision research and has been optimized within the context of feature detections in medical imaging. Frangi et al. (1998) and Sato et al. (1998) presented its operation for the specific situation of detecting the web of blood vessels in a medical image, a notoriously complex pattern of elongated

tenuous features whose branching make it closely resemble a fractal network. Aragón-Calvo et al. (Aragón-Calvo et al. 2006) translated, extended and optimized this technology towards the recognition of the major characteristic structural elements in the Megaparsec matter distribution of a method finding its origin in computer vision research.

The first applications to the galaxy distribution in the Sloan Digital Sky Survey produced a spectacular result: an objective cluster and filament catalog. Equally encouraging were the results of an application to a modelled galaxy distribution in the Millennium Simulation.

7 Acknowledgement

The author would like to thank Dick Bond for many years of inspiration and encouragement in studying the cosmic web and constrained fields. I am grateful to both Bernard Jones and Manolis Plionis for providing substantial feedback on various relevant issues. In addition, Willem Schaap and Miguel Aragón-Calvo are acknowledged for essential contributions to the presented work.

References

Aragón-Calvo, M., van de Weygaert, R., & van der Hulst, J.M., 2006, Astron. Astrophys., submitted

Bertschinger, E., 1987, Astrophys. J., 323, 103

Bond, J.R., & Myers, S.T., 1996, Astrophys. J. Suppl., 103, 41

Bond, J.R., Kofman, L., & Pogosyan, D., 1996, Nature, 380, 603

Colberg, J.M., Krughoff, K.S., & Connolly, A.J., 2005, MNRAS, 272

Eisenstein, D.J., & Loeb, A., 1995, Astrophys. J., 439, 520

Frangi A., Niessen, W.J., Vincken, K.L., & Viergever, M.A., Lecture Notes in Computer Science, 1496, 130

Hoffman, Y., & Ribak, E., 1991, Astrophys. J., 380, 5

Hui, L., & Bertschinger, E., 1996, Astrophys. J., 471, 1

Icke, V., 1973, Astron. Astrophys., 27, 1

Jain, B., & Bertschinger, E., 1994, Astrophys. J., 431, 486

Jones, B.J.T., & Van de Weygaert, R., 2006, in prep.

Kang, H., Ryu, D., Cen, R., & Song, D., 2005, Astrophys. J., 620, 21

Kang, H., 2006, in *Measuring the Warm-Hot Intergalactic Medium*, workshop proceedings, ed. Yamasaki, N.Y., den Herder, J-W, Suto, Y., Yoshikawa, K., 2006

Klypin, A., Hoffman, Y., Kravtsov, A.V., & Gottlöber, S., 2003, Astrophys. J., 596, 19

Mathis, H., Lemson, G., Springel, V., Kauffman, G., White, S.D.M., Eldar, A., & Dekel, A., 2002, MNRAS, 333, 739

Sambridge, M., Braun, J., & McQueen, H., 1995, Geophys. J. Int., 122, 837

Sathyaprakash, B.S., Sahni, V., & Shandarin, S.F., 1996, Astrophys. J., 462, 5

Sato, Y., Nakajima, D., Atsumi, H., et al., 1998, IEEE Medical Image Analysis 2,2,143

Schaap, W., 2006, *the Resolving Patterns in the Universe: the Delaunay Tessellation Field Estimator*, Ph.D. thesis, University of Groningen

Schaap, W., & van de Weygaert, R., 2000, Astron. Astrophys., 363, L29

Sheth, R., 1995, MNRAS, 277, 933

Sibson, R., 1980, Math. Proc. Camb. Phil. Soc., 87, 151

Sibson, R., 1981, in *Interpreting Multivariate Data*, p. 21, ed. Barnet V., Wiley, Chichester

Sukumar, N., 1998, Sukumar, N., *The Natural Element Method in Solid Mechanics*, Ph.D. thesis, Northwestern University

Van de Weygaert, R., & Bertschinger, E., 1996, MNRAS, 281, 84
Van de Weygaert, R., 2002, in *Modern Theoretical and Observational Cosmology*, proceedings 2nd Hellenic Cosmology Meeting, ed. M. Plionis, S. Cotsakis, ASSL 276, p. 119, Kluwer
Watson, , 1992,
Zaroubi, S., Hoffman, Y., Fisher, K.B., & Lahav, O., Astrophys. J., 449, 446
Zel'dovich, Ya.B., 1970, Astron. Astrophys., 5, 84